LIMNOLOGY
and
OCEANOGRAPHY

ASLO

Limnol. Oceanogr. 61, 2016, 825–840

doi: 10.1002/lno.10261

Meso- and microzooplankton grazing in the Amazon River plume and western tropical North Atlantic

Brandon J. Conroy,*[1] Deborah K. Steinberg,[1] Michael R. Stukel,[2] Joaquim I. Goes,[3] Victoria J. Coles[4]

[1]Department of Biological Sciences, Virginia Institute of Marine Science, College of William and Mary, Gloucester Point, Virginia

[2]Department of Earth, Ocean, and Atmospheric Science, Florida State University, Tallahassee, Florida

[3]Lamont Doherty Earth Observatory, Columbia University, Palisades, New York

[4]Horn Point Laboratory, University of Maryland Center for Environmental Science, Cambridge, Maryland

Abstract

Largely due to size differences, mesozooplankton are important exporters of carbon and prey for larger organisms, while microzooplankton are important recyclers of nutrients, dominant grazers of phytoplankton, and a key link in the microbial loop. We investigated the relative importance of meso- and microzooplankton grazing in the western tropical North Atlantic Ocean (WTNA) and Amazon River plume. Sampling as part of the ANACONDAS project occurred in spring (May–June) 2010 during the peak outflow of the Amazon River and in fall (September–October) 2011 during the plume seasonal retroflection. Mesozooplankton grazing rates decreased with increasing salinity in both seasons, but during the fall both day and nighttime grazing rates were significantly negatively correlated with salinity. Mesozooplankton grazing was highest in plume-influenced surface waters (0–25 m), and usually dominated by smaller size classes (0.2–0.5 mm and 0.5–1.0 mm). Microzooplankton grazing accounted for approximately 68% of bulk phytoplankton growth across all stations. Comparison of meso- and microzooplankton grazing suggests a transition in food web dynamics from a mesozooplankton dominated "export" structure in the plume transitioning to a microzooplankton dominated "retention" structure at mesohaline and oceanic stations above sea surface salinity of 33. Comparison between the seasons suggests a seasonal planktonic succession of low mesozooplankton grazing during the spring peak discharge followed by higher grazing rates and impact by mesozooplankton during the fall retroflection. These results provide important baseline information required for examining effects of climate change on the planktonic food web of the WTNA and for use in biogeochemical models of the region.

The role that zooplankton play in determining the structure and efficiency of pelagic food webs varies with a multitude of factors, including region, season, depth, and phytoplankton and zooplankton size. Retention food webs are considered characteristic of open ocean, oligotrophic environments, where microzooplankton efficiently graze small phytoplankton, and nutrients and organic material are retained and recycled in surface waters (Wassmann 1997). Export food webs on the other hand, common to upwelling or coastal regions, are characterized by large phytoplankton and shorter food webs, with phytoplankton sinking out in aggregates or grazed by large zooplankton producing rapidly sinking fecal pellets (Michaels and Silver 1988; Wassmann 1997; Stukel et al. 2013b). This study investigates meso- and microzooplankton grazing in a region where these two food web paradigms potentially overlap, due to the mingling of the nutrient rich outflow of the Amazon River with the oligotrophic western tropical North Atlantic Ocean (WTNA).

In the WTNA, the Amazon River flows onto the shelf, forming a thin, low salinity and high nutrient plume with very strong vertical stratification. The plume creates a unique environment for enhanced primary production driven primarily by diazotrophy (N_2-fixation) from diatom-diazotroph associations (DDAs) (Subramaniam et al. 2008). The plume covers up to 1.5×10^6 km^2 of the WTNA in July and August during the period of retroflection when the North Equatorial Countercurrent surfaces and advects fresh water eastward across the basin (Molleri et al. 2010; Coles et al. 2013). Earlier in the spring, in May and June, the plume is primarily flowing northwestward, although the retroflection may initiate toward the end of this period. The plume ranges from

*Correspondence: bconroy@vims.edu

This article was published online on 30 January 2016. An error was subsequently identified. This notice is included in the online and print versions to indicate that both have been corrected 24 February 2016.

5 m to 25 m thick (Coles et al. 2013) and supplies allocthonous silicon (Si) and phosphorus (P) to offshore regions of the WTNA. This input of plume Si and P into the nitrogen-limited open ocean at Si : N and P : N ratios in excess of that typically needed by phytoplankton creates a distinct niche for N_2 fixation by DDAs, leading to enhanced primary production in this region (Subramaniam et al. 2008). Carbon drawdown associated with this primary production challenges the previous view of the tropical ocean as a source of carbon to the atmosphere (Takahashi et al. 2002; Mikaloff-Fletcher et al. 2007) and instead affirms that the region is a biologically-mediated carbon sink (Cooley and Yager 2006; Cooley et al. 2007; Subramaniam et al. 2008).

The fate of this enhanced production in the WTNA, however, is unknown. Aside from a historical study in this region that quantified copepods and cladocerans in the surface 200 m (Calef and Grice 1967), characterization of zooplankton community composition has been restricted to the Amazon River coastal estuaries (Costa et al. 2009; Magalhães et al. 2009). Furthermore, there are no previous studies describing zooplankton grazing in the plume-influenced WTNA. Most studies of mesozooplankton grazing in the tropical open ocean have been limited to the Pacific Ocean, i.e., the Joint Global Ocean Flux Study (JGOFS) Equatorial Pacific study (EqPac) (Dam et al. 1995; Zhang et al. 1995; Roman and Gauzens 1997; Roman et al. 2002), and more recently the Equatorial Biocomplexity project (Décima et al. 2011; Landry et al. 2011). In the Atlantic Ocean, tropical mesozooplankton grazing is limited to the eastern portion of the basin, where results from the Atlantic Meridional Transect project indicate mesozooplankton grazing impact averaged 2.3% of chlorophyll *a* (Chl *a*) (Isla et al. 2004) in the eastern tropical North Atlantic and an average of 6% of Chl *a* in the subtropics near the Azores (Huskin et al. 2001).

Likewise, little is known about the impacts of microzooplankton grazing in the WTNA. Small protozoa are considered to be the dominant grazers globally, accounting for removal of 70–133% of primary production per day (Sherr and Sherr 2002) and 75% overall in the tropical and subtropical regions as determined by metadata analysis (Calbet and Landry 2004). A subsequent metadata analysis of microzooplankton grazing, using Longhurst's classic biogeographic domains and an expanded dataset (nearly double the data points of the 2004 study), indicates that within the "Trades Atlantic" region, microzooplankton grazing accounts for approximately 70% of primary production grazed per day (Schmoker et al. 2013). However, this biogeographic region, which includes the WTNA, was specifically recommended for further study of microzooplankton grazing, as the only open ocean study was located near the Azores, with the remaining coming from subtropical or tropical estuaries (Schmoker et al. 2013).

Here we attempt to quantify meso- and microzooplankton grazing in the Amazon-influenced WTNA to address a distinct gap in our understanding of the fate of the enhanced primary production in this region. We also provide an important baseline of removal of primary production in the different water types of the WTNA under current climate conditions. Observed changes to the hydrological cycle in the Amazon basin (Gloor et al. 2013) and increasing temperature predicted with climate change (Doney et al. 2012) could directly impact the Amazon River discharge which is linked with both the El Niño Southern Oscillation (ENSO) and sea surface temperature in the tropical north Atlantic (Richey et al. 1989; Espinoza et al. 2011). Furthermore, these measurements will improve existing empirical and biogeochemical models of this dynamic region (Cooley et al. 2007; Stukel et al. 2014), as well as provide important comparisons with other major rivers discharging into the oceans (e.g., the Mississippi, Mekong, and Congo).

Methods

Study area

Sampling in the Amazon River plume-influenced region of the WTNA (between 0–13°N and 44–57°W) was conducted as part of the Amazon iNfluence on the Atlantic: CarbOn export from Nitrogen fixation by DiAtom Symbioses (ANACONDAS) project. We report data from two cruises which occurred 22 May 2010–24 June 2010 aboard the R/V *Knorr* and 03 September 2011–08 October 2011 aboard the R/V *Melville*. The cruise in 2010, hereafter referred to as "spring," focused on the plume during the season of peak discharge (Fig. 1A), and in 2011, referred to as "fall," during the seasonal maximum reach and plume retroflection that advects the plume southeastward (Fig. 1B). Sampling design included stations in and out of the plume to capture variation in biogeochemistry with respect to plume influence. Station selection was based largely on sea surface salinity (SSS) and Chl *a* and phycobilipigment fluorescence measured underway (Goes et al. 2014), and other plume indicators (e.g., chromophoric dissolved organic matter-CDOM concentration) seen from satellite imagery. For the purposes of this analysis, we separate sampling stations into the following categories: stations with SSS < 30 were identified as "low salinity" plume, stations with SSS between 30 and 35 "mesohaline" plume, and stations with SSS > 35 "oceanic" non-plume.

Mesozooplankton collection

Mesozooplankton (i.e., zooplankton > 0.2 mm) were collected in both years with a 1-m Multiple Opening and Closing Net and Environment Sensing System (MOCNESS; Wiebe et al. 1976) fitted with ten 202 μm mesh nets. Tows were performed to 150 m or 500 m. Only the 0–150 m depth intervals were processed for determination of gut fluorescence to avoid problems with gut evacuation and pigment degradation during the tow, and were always sampled last in the tow. Discrete depth intervals within the top 150 m were 0–25 m, 25–50 m, 50–100 m, and 100–150 m during the spring. In the fall, to better characterize the surface plume influence, we sampled

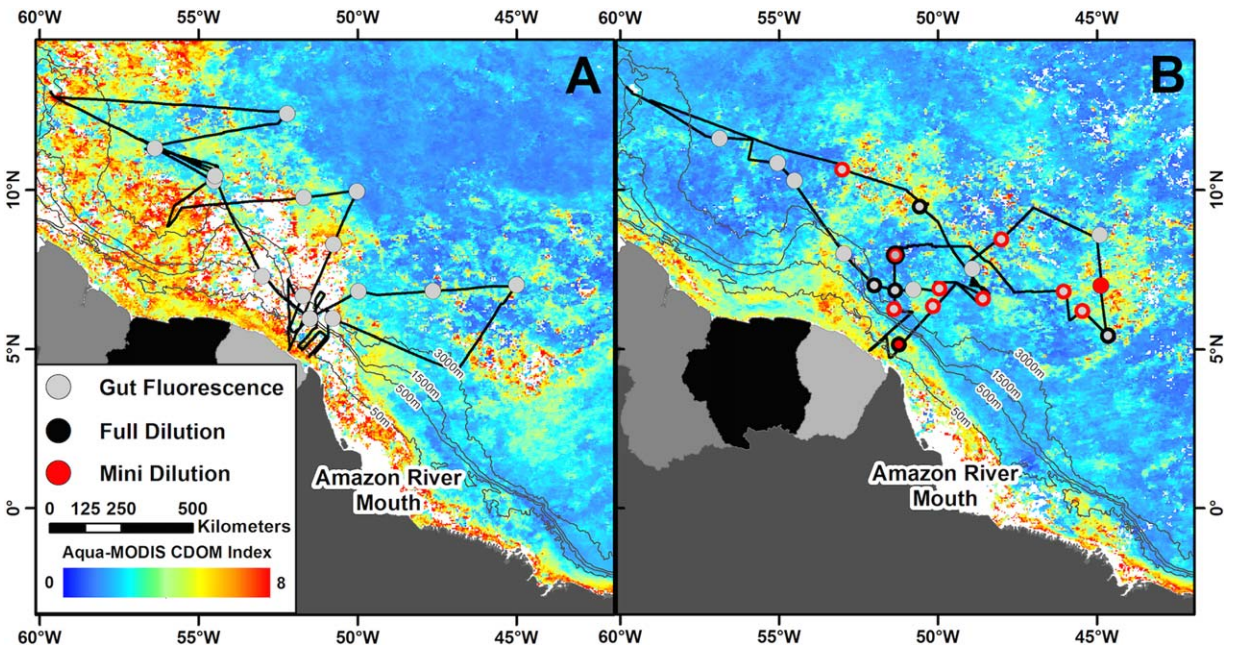

Fig. 1. Stations sampled for mesozooplankton gut fluorescence and microzooplankton grazing in the Amazon River plume-influenced waters and the western tropical North Atlantic. Stations with cruise track (black line) are overlaid on monthly averaged chromophoric dissolved organic matter (CDOM) concentration using Aqua-MODIS satellite data (oceancolor.gsfc.nasa.gov). (**A**) Stations sampled in spring (May–June) 2010 during the Amazon River peak discharge. (**B**) Stations sampled in fall (September–October) 2011 during the seasonal maximum areal reach of the plume. Station color or combination of colors indicates sampling protocol performed at that station. Bathymetry lines are shown in gray.

the top 25 m at higher resolution (0–10 m and 10–25 m; deeper intervals remained the same as in spring). Occasionally, at shallow depth stations, a double oblique tow using a rectangular frame (0.8 × 1.2 m) single net with 202 μm mesh was performed in surface waters (within top 25 m). When possible, both day and night tows were performed. Daytime tows were performed between 1000 h and 1400 h local time and nighttime tows between 2200 h and 0200 h. Once the nets were onboard, zooplankton in the cod ends used for pigment analysis were immediately anesthetized with carbonated water to prevent gut evacuation (Gannon and Gannon 1975). Samples were then split into either 1/4 or 1/2 of the total sample using a Folsom plankton splitter, then size fractionated using nested sieves into the following size classes: 0.2–0.5 mm, 0.5–1.0 mm, 1.0–2.0 mm, 2.0–5.0 mm, and > 5.0 mm. These size fractions were then concentrated onto pre-weighed, 0.2 mm Nitex mesh filters and rinsed with Milli-Q to remove salt. When large phytoplankton were caught in the nets, filters were first inspected and picked clean of phytoplankton, then the filters were placed in petri dishes and frozen and stored at −80°C until they were processed on shore.

Gut fluorescence analysis and mesozooplankton grazing calculation

Gut fluorescence for each size fraction was determined fluorometrically similar to that described in (Décima et al. 2011). For the 0.2–0.5 mm, 0.5–1.0 mm, 1.0–2.0 mm, and 2.0–5.0 mm size fractions, replicate 1/8 or 1/4 sections of the frozen filter were processed. Filters were sectioned in equal divisions using a sectioning template. On occasions when the 2.0–5.0 mm size fraction contained very low biomass, and always for the > 5 mm size fraction, the entire filter was processed. The samples were sonicated in 90% acetone and extracted for 2 h. Samples were then centrifuged to settle particulates, and concentrations of Chl *a* and phaeopigments (Phaeo) in the supernatant were measured in either a Turner TD-700 or Trilogy fluorometer pre-calibrated using standing Chl *a* (Parsons et al. 1984; Båmstedt et al. 2000). As suggested by Conover et al. (1986), we did not multiply the Phaeo values by a factor of 1.51, because standard fluorometric procedures express the values as chlorophyll weight equivalents already.

For each discrete depth interval the total pigment concentration was calculated as:

$$\mathrm{GPC} = \frac{pig \times \left(\frac{1}{split}\right) \times \left(\frac{1}{f}\right)}{vol} \quad (1)$$

where GPC is gut pigment content (mg m^{-3}), *pig* is the sum of the Chl *a* and Phaeo values (mg), *split* is the fraction of total tow, *f* is the fraction of filter analyzed and *vol* is the volume of water filtered through the net (m^{-3}).

Ingestion (grazing) rates (mg Chl *a* equiv. m^{-3} d^{-1}) were calculated as:

$$I = \mathrm{GPC} \times k \quad (2)$$

where GPC is gut pigment content (mg m^{-3}) and k is the daily gut evacuation rate (d^{-1}). We estimated a k value for all nets using the temperature dependent function k (d^{-1}) = (0.0124 $e^{0.0765T(°C)}$) × 1440 min d^{-1} from (Dam and Peterson 1988). For tows using the MOCNESS the average temperature of each depth interval was used to calculate k. For occasional oblique tows with a single net in the surface 25 m, surface temperature was used to calculate k. We chose a temperature-dependent formula to determine k to reflect grazing rate changes with decreasing temperature and increasing depth, rather than apply an average k determined from equatorial waters that shows somewhat lower k at higher temperature than would be predicted by Eq. 2 (Zhang et al. 1995). Following the recommendation of Durbin and Campbell (2007), and the procedure used in recent studies (Landry et al. 2009; Décima et al. 2011; Bernard et al. 2012), we calculated grazing rates without the gut pigment degradation value previously included in grazing rate equations (Båmstedt et al. 2000).

Mesozooplankton grazing impact (%) was calculated for Chl *a* in the top 150 m of the water column. Chl *a* was measured following the standard fluorometric methods outlined by the JGOFS program (Knap et al. 1996) and trapezoidally integrated to 150 m. Briefly, 0.5–1.0 L of seawater from the CTD rosette was vacuum filtered onto a 25 mm GF/F filter. Filters were then placed in 90% acetone and allowed to extract for 4 h. They were then measured onboard using a Turner Trilogy fluorometer before and after acidification with two drops of 1.2 M HCl. Grazing rates were also depth integrated by multiplying I (mg m^{-3} d^{-1}) by the appropriate depth interval for each MOCNESS net then summing the nets from each tow. For oblique tows, grazing rates were multiplied by the maximum depth of the net.

We note several potential sources of error in the gut fluorescence method. As in our analysis, many previous studies assume that pigment degradation is accounted for in experimental determination of k (Durbin and Campbell 2007; Landry et al. 2009; Gleiber et al. 2015). However, the study of Karaköylü and Franks (2012) using in vivo gut fluorescence in copepods found traditional gut evacuation rate experiments may underestimate grazing by 15–70%, which they attributed largely to differences between copepod feeding state (i.e., they measured gut fluorescence during active feeding). Furthermore, sampling bias from using a 202 μm net may have occurred between our mesozooplankton and microzooplankton collection creating a "grey zone" in our data potentially excluding organisms from roughly 100–450 μm (Hopcroft et al. 2001). These sources of error lead to potential underestimation of grazing rates and our estimates should therefore be considered conservative.

Microzooplankton grazing

In the fall, we conducted two types of experiments to measure phytoplankton growth and protozoan grazing rates: full serial dilution series (Landry and Hassett 1982) at surface depths and two-point "mini" dilutions (Landry et al. 1984, 2008) to determine depth profiles of grazing. All samples were taken from a Niskin rosette and incubated in 2.2 or 1-L polycarbonate bottles. All incubations were carried out for 24 h in deck-board incubators maintained at surface temperatures by a flow-through seawater system. Bottles were screened with black mesh to hold them at in situ light levels.

Serial dilutions

Serial dilutions were carried out at surface depths to confirm that grazing pressure decreased linearly with dilution. Duplicate treatments were set up at dilution levels of 24%, 37%, 61%, and 73% whole seawater, and amended with 200 μL of 100 mM NH_4^+ and 50 mM PO_4^{3-} (final concentrations were 8.5 μM and 4.3 μM, respectively). Nutrients were added to ensure that a reduction in nutrient cycling in treatment bottles would not alter phytoplankton growth rates. Four control bottles were also set up (100% whole seawater), including two nutrient-amended replicates and two natural replicates. All treatment bottles were prepared by first filtering water with a peristaltic pump directly from the Niskin bottle through a 0.1 μm Acropak filter cartridge and into a known volume bottle of appropriate size for the respective dilution. Filtered water was then poured into a 2.2-L clear polycarbonate incubation bottle. The incubation bottle was then gently filled the rest of the way with whole seawater from the Niskin using silicon tubing. Net growth rates for each bottle were calculated from initial and final Chl *a* concentrations as: $k_{net} = \ln(chl_{final}/chl_{init})$. Net growth rates of all nutrient-amended treatments were then regressed on dilution factor and the slope (equal to grazing rate) and y-intercept (equal to nutrient-amended gross growth rate) were calculated using a type I linear regression. Ambient phytoplankton gross growth rates were then calculated as the sum of grazing rate (i.e., slope) and the net growth rate of non-nutrient amended whole seawater samples.

Two-point dilutions

Two point dilutions were set up similarly to the serial dilutions described above, except that only two bottles were used (37% treatment level and whole seawater) and were not nutrient amended. Two-point dilutions were not nutrient-amended so that we could determine natural phytoplankton growth rates. Typically we conducted four sets of two-point dilutions at light levels of 33%, 11%, 4%, and 1% surface irradiance. Grazing rate was calculated as $(k_{dilute}\text{-}k_{whole})/0.63$ and gross growth rate was calculated as k_{whole} + grazing rate.

Microzooplankton and mesozooplankton instantaneous grazing rate comparisons

To compare the daily impact of micro-and mesozooplankton grazing on phytoplankton, mesozooplankton grazing rates were converted to instantaneous grazing rates (d^{-1}) by the equation:

$$\ln\left(\frac{\mathrm{Chl_D} - I_D}{\mathrm{Chl_D}}\right) \quad (3)$$

where $\mathrm{Chl_D}$ and I_D are depth-integrated chlorophyll (mg Chl *a* m^{-2}) and grazing (mg Chl *a* equiv. m^{-2} d^{-1}), respectively. When night and day values of grazing were available, values were reported as total mesozooplankton impact (M_{TOT} d^{-1}) and I_D was calculated as:

$$\frac{\Sigma(I_{DAY} + I_{NIGHT})}{2} \quad (4)$$

so that Eq. 2 was corrected for 12 h of daytime grazing and 12 h of nighttime grazing. If only day tows were available, values are reported as daytime mesozooplankton impact (M_{DAY}, d^{-1}) and only I_{DAY} (i.e., for 24-h period) was used to calculate I_D. Mesozooplankton grazing was integrated to the nearest possible depth interval to the corresponding two-point microzooplankton depth profiles (i.e., to depth of 1% light level; average of 70 m for all experiments but ranged from 25 m to 120 m, depending on station).

Statistical analyses

Data were analyzed using SigmaPlot 11.0. Integrated grazing rates were regressed against salinity for both night and day tows. Comparisons between seasons were made with unpaired *t*-tests while comparisons between station categories for the same seasons were analyzed using one-way ANOVA. When data did not meet expectations of equal variance and normality, they were ranked and analyzed using non-parametric tests. These included the Mann–Whitney rank sum test for between season comparisons, and the Kruskal–Wallis ANOVA on ranks for comparison between station categories.

Statistical significance of serial microzooplankton dilution experiments was determined using a Type I linear regression. To determine the uncertainties for two-point "mini" dilutions, we made the assumption that the full serial dilutions yielded accurate growth and grazing rates, then calculated the apparent growth and grazing rates that would have been determined from using only a single pair of 37% and 100% whole seawater treatments from the full dilutions. The mean differences between the full dilution and two-point dilution growth and grazing measurements were -0.02 ± 0.11 and 0.001 ± 0.13 d^{-1}, respectively (mean ± standard error), suggesting that the two-point dilutions do not bias either growth or grazing rate measurements. We calculated the root mean square errors to estimate the uncertainty of any particular two-point growth or grazing rate measurement to be 0.21 d^{-1} and 0.24 d^{-1}, respectively. These uncertainty estimates were then propagated through future calculations to determine the measurement uncertainty associated with using the two-point dilution technique.

Results

Seasonal and regional depth-integrated mesozooplankton grazing patterns

Mean mesozooplankton grazing rates (integrated from 0 m to 150 m) for all salinities combined were ~ 2 to 2.4-fold higher in fall than spring during the day (2.49 vs. 1.15 mg Chl *a* equiv. m^{-2} d^{-1}, fall vs. spring, respectively) and night (2.39 vs. 0.99 mg Chl *a* equiv. m^{-2} d^{-1} fall vs. spring) (Table 1). Mean values for comparison between seasons of all salinities did not meet assumptions of normality but median grazing rates for both night and day were significantly different and higher in the fall ($p = 0.03$ for daytime rates and $p = 0.04$ for nighttime).

During both years mesozooplankton grazing generally decreased as salinity increased (Fig. 2). In spring, daytime grazing rates ranged from 0.24 to 4.02 mg Chl *a* equiv. m^{-2} d^{-1} and nighttime rates ranged from 0.27 to 2.70 mg Chl *a* equiv. m^{-2} d^{-1}; neither nighttime nor daytime grazing rates were significantly different across the salinity range (Fig. 2A). In fall, daytime grazing rates ranged from 0.31 to 11.34 mg Chl *a* equiv. m^{-2} d^{-1}, and nighttime rates ranged from 0.33 to 8.99 mg Chl *a* equiv. m^{-2} d^{-1}; both daytime and nighttime grazing significantly decreased with increasing surface salinity (Fig. 2B).

Spatial patterns in mesozooplankton grazing were evident when the expanse of the plume was examined. During spring the plume extended northwestward and was sampled to approximately 14°N, with the highest grazing at low salinity plume stations on the continental shelf or on the slope (Fig. 3A,B). Grazing rates were low outside of the core plume region with two exceptions: a station located northwest in the outer plume (daytime and nighttime grazing rates were 0.71 and 2.7 mg Chl *a* equiv. m^{-2} d^{-1}, respectively), and a deep, open ocean station (daytime grazing rate of 1.6 mg Chl *a* equiv. m^{-2} d^{-1}). During fall we observed a similar pattern of grazing, although rates were two to three times higher and more strongly correlated with surface salinity compared with spring. Grazing was highest in the same low salinity shelf and slope region as in spring but was also elevated within the outer plume retroflection (Fig. 3C,D). In the outer most portion of the retroflection, grazing rates ranged from 1.9 to 4.0 mg Chl *a* equiv. m^{-2} d^{-1} during the daytime, and reached 3.7 mg Chl *a* equiv. m^{-2} d^{-1} at night. The other region of elevated grazing was in the farthest northwest station with respective day and night grazing rates of 2.9 and 3.6 mg Chl *a* equiv. m^{-2} d^{-1} (Fig. 3C,D).

Mesozooplankton grazing depth profiles

Patterns of grazing with depth were similar between seasons, and are illustrated for the fall in Fig. 4. Highest grazing occurred in surface waters at low salinity, plume stations, with higher grazing rates shifting to deeper in the water column as surface salinity increased (Fig. 4). At plume stations, the highest grazing rates were concentrated in the top 25 m

Table 1. Depth integrated (0–150 m) mesozooplankton grazing rates (mg Chl *a* equivalent m^{-2} d^{-1}) in spring (May–June) 2010 and fall (September–October) 2011. Values are averages ± 1 standard deviation for each year by station category and day or night tow.

Season	Station category	Day	Night
Spring	Low salinity plume	1.60 ± 1.72 ($n = 4$)	1.08 ($n = 1$)
	Mesohaline plume	1.05 ± 0.97 ($n = 5$)	1.08 ± 1.00 ($n = 5$)
	Oceanic	0.82 ± 0.55 ($n = 4$)	0.82 ± 0.27 ($n = 3$)
	Total	1.15 ± 0.31 ($n = 13$)	0.99 ± 0.24 ($n = 9$)
Fall	Low salinity plume	5.34 ± 4.13 ($n = 4$)	6.87 ($n = 1$)
	Mesohaline plume	1.96 ± 1.46 ($n = 14$)	2.46 ± 1.25 ($n = 7$)
	Oceanic	0.48 ($n = 2$)	0.76 ± 0.53 ($n = 3$)
	Total	2.49 ± 0.57 ($n = 20$)	2.39 ± 0.59 ($n = 11$)

where plume influence was strongest (Fig. 4A,D); at mesohaline stations grazing rates followed a similar pattern although rates were not as high. Open ocean stations were characterized by lower grazing rates throughout the water column (an order of magnitude lower than at plume stations) with a slight peak at depth corresponding to a deep chlorophyll max (Fig. 4C,F). This pattern is also apparent in a transect through the plume during the fall cruise which starts on the periphery of the plume and ends in the open ocean (Fig. 5).

Across all stations and nearly all depth intervals the highest grazing rates were in the smallest size fractions of mesozooplankton (0.2–0.5 mm and 0.5–1.0 mm) (Fig. 4). A notable exception occurred whereby daytime grazing rates for the 1.0–2.0 mm size fraction at oceanic stations exceeded the smaller size fractions at depths of 50–100 m and 100–150 m (Fig. 4C), near the depth of the Chl *a* maximum (Fig. 4F). Calanoid copepods dominated mesozooplankton abundance in nearly all depths, size fractions, and salinities, with cyclopoid and poecilostomatoid copepods only occasionally exceeding abundance of calanoids. Rare exceptions to copepod dominance occurred in larger size fractions (usually > 2.0 mm) where decapod larvae and shrimp (e.g., families Sergestidae and Luciferidae, respectively) were prevalent in the surface plume layers.

Mesozooplankton grazing impact

In spring average mesozooplankton grazing impact across all salinities on phytoplankton standing stock was 2.3% during the day and 1.9% at night, compared with 7.1% and 6.0% for day and night, respectively, in the fall (Table 2). Mean values across all salinities were non-normal but the median was significantly higher in fall ($p = < 0.001$). Mean values of both mesohaline day ($p = 0.038$) and night ($p = 0.003$) grazing impact were significantly higher in fall than spring.

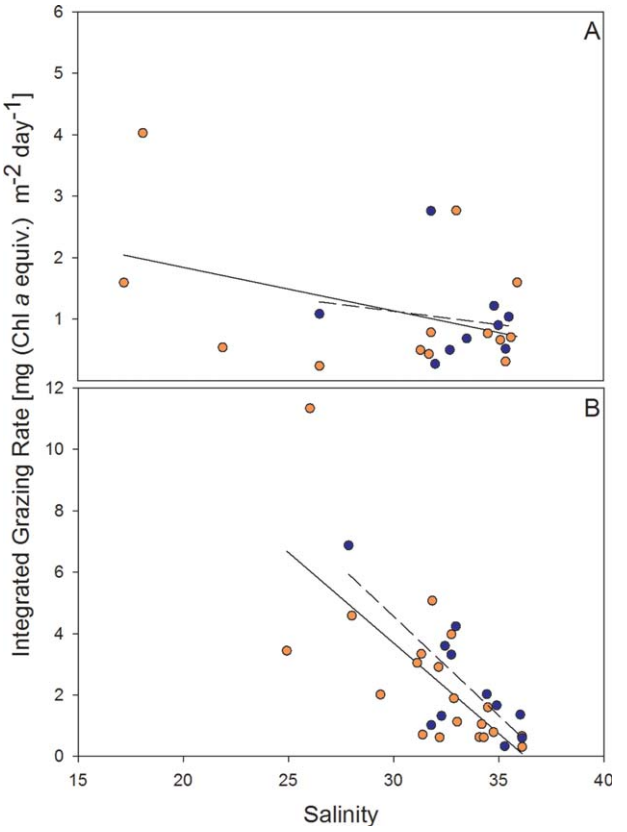

Fig. 2. Surface salinity vs. mesozooplankton grazing (0–150 m integrated) during day (orange) and night (blue) in (**A**) spring, and (**B**) fall. Regression lines are shown separately for day (solid) and night (dashed). Note that the *y*-axis (grazing) scale in **B** is double that in **A**. Regression equations and statistics are as follows: (**A**) day, $n = 13$, $y = -0.0708x + 3.258$, $p = 0.146$ $R_2 = 0.182$; night, $n = 9$, $y = -0.0436x + 2.4333$, $p = 0.665$, $R_2 = 0.0283$; (**B**) day, $n = 20$, $y = -0.590x + 21.382$, $p = < 0.001$, $R_2 = 0.491$; night, $n = 11$, $y = -0.646x + 23.937$, $p = 0.004$, $R_2 = 0.627$.

To further explore grazing within the plume we also determined mesozooplankton grazing impact in the top 25 m only (Table 2). The average daytime grazing impact in fall was almost 10-fold that in spring, while nighttime grazing impact was ~ 3 times higher. Mean values were non-normal but median values were significantly higher across all stations ($p < 0.001$), for daytime mesohaline ($p = 0.004$) and plume ($p = 0.029$) stations in fall compared with spring.

Microzooplankton grazing rates

In the fall, we conducted a total of 7 serial dilutions and 55 two-point, "mini" dilutions. We compared the full dilutions and mini dilutions to confirm linearity of both phytoplankton growth and microzooplankton grazing between the two methods. Both were linear, although grazing was more variable, and we report mini dilution results below.

From the mini-dilutions, microzooplankton grazing was strongly positively correlated with bulk phytoplankton growth (Fig. 6). Across the range of conditions sampled,

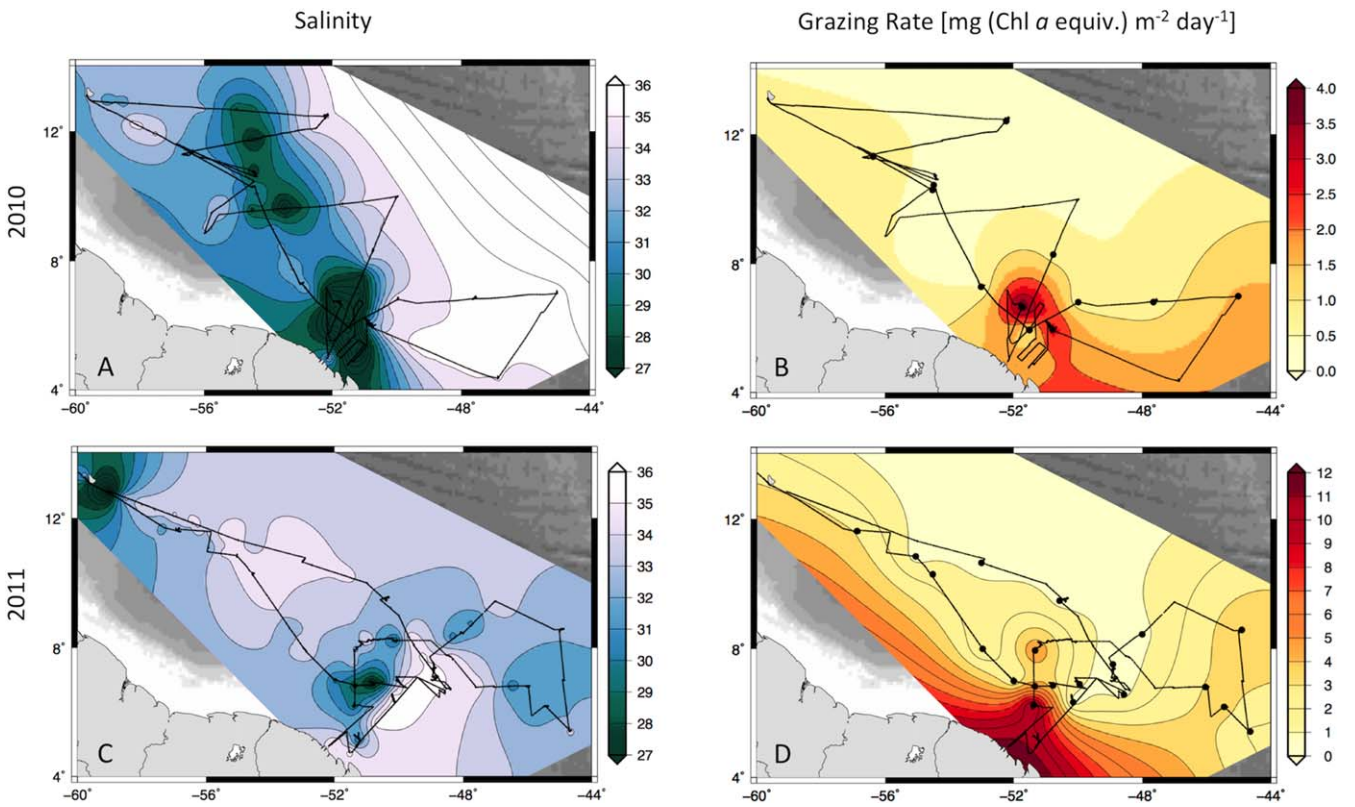

Fig. 3. Surface salinity and daytime mesozooplankton grazing (0–150 m integrated) in spring (**A** and **B**, respectively) and fall (**C** and **D**, respectively) in the Amazon River plume region. Note the scale in **D** is triple that in **B**.

protozoan grazing averaged 68% of phytoplankton growth. Neither phytoplankton growth nor microzooplankton grazing was significantly correlated to sea surface salinity. There was no statistically significant trend of phytoplankton growth or microzooplankton grazing with level of photosynthetically active radiation (PAR), although generally phytoplankton growth was suppressed in surface waters where PAR was highest and then increased and peaked at light levels approximately 10% of surface irradiance (Fig. 7A). Microzooplankton grazing was not inhibited at high PAR but did decrease as light levels decreased in the same way as phytoplankton growth (Fig. 7B). We note that samples collected at depth were incubated at temperatures higher than ambient for their respective depth due to variation in the thermocline. This likely did not lead to significant overestimation of grazing rates, which at depth were consistently the lowest observed.

Comparison of mesozooplankton and microzooplankton grazing impact

A total of nine stations were available to compare the relative importance of microzooplankton and mesozooplankton grazing on phytoplankton growth (μ) across the plume (Fig. 8). Of the four lowest salinity stations (12, 25, 19, and 20) the net calculated change (k') was negative for all except station 25. At all four of these stations μ did not exceed 0.6 d^{-1}. Of these low salinity stations, mesozooplankton grazing impact exceeded that of microzooplankton at all but station 25. For the remaining mesohaline and oceanic stations (13, 8, 26, 9, and 10) that pattern was reversed, with a positive k' and only one value for μ below 0.6 d^{-1}. At the highest salinity, oceanic stations, microzooplankton grazing impact was 2–13 times higher than that of mesozooplankton.

Discussion

Grazing patterns

Plume stations

The highest mesozooplankton grazing rates in spring were concentrated in the low salinity plume, a region characterized by an "estuarine type" phytoplankton assemblage consisting of a high abundance of diatoms, cryptophytes, and green-water *Synechococcus* spp. (Goes et al. 2014). This was also the only region with detectable nitrate and nitrite, and contained the highest concentrations of silicate (Goes et al. 2014). During the fall plume retroflection, the highest grazing rates at the low salinity plume stations occurred in nearly the same geographic region although the rates were double to triple those in spring (Fig. 3). A similar diatom-dominant phytoplankton assemblage with *Chaetoceros* spp.,

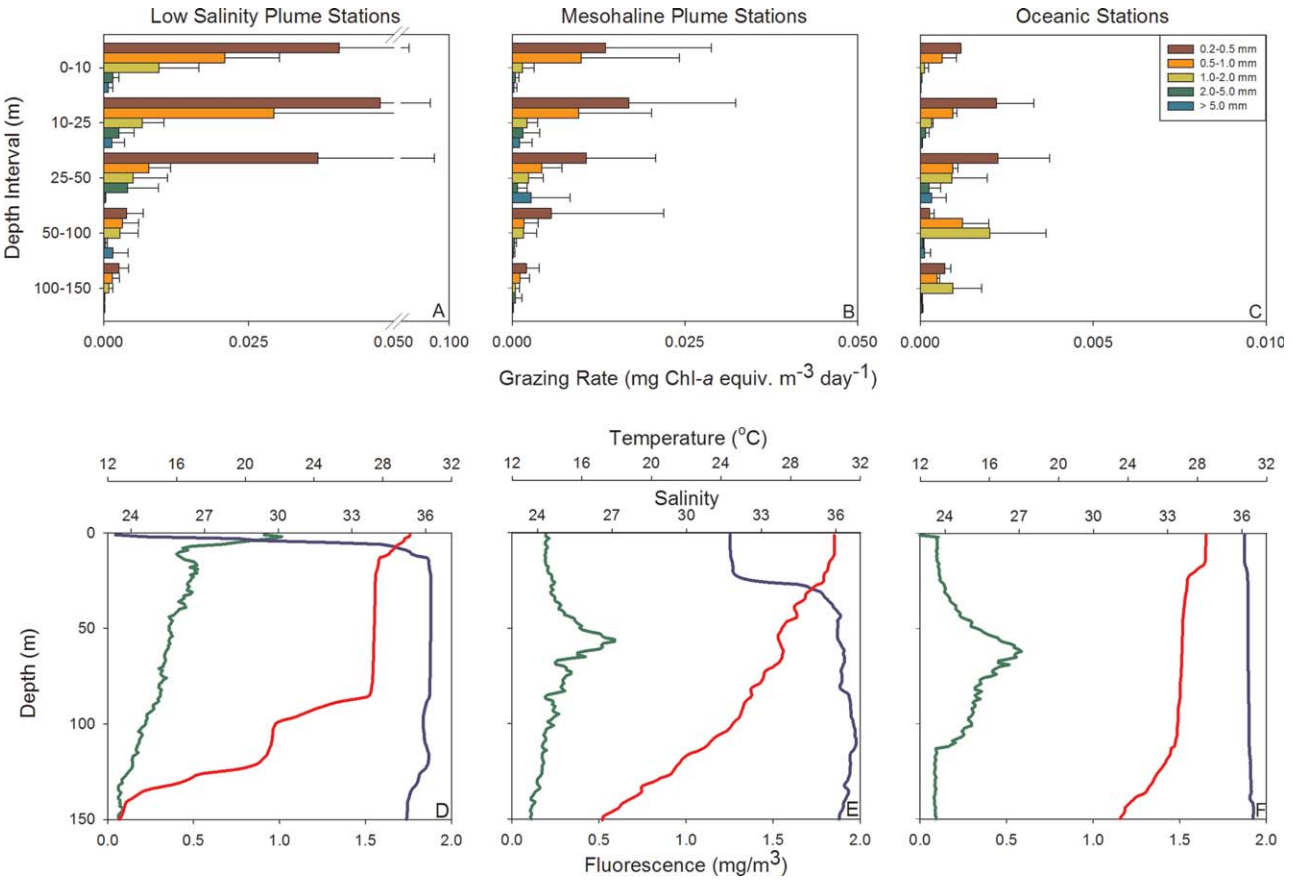

Fig. 4. Size-fractionated mesozooplankton daytime grazing (**A**–**C**) depth profiles in fall averaged by salinity category, size class, and depth interval. Error bars are standard deviation. Note different *x*-axis scales. **D**–**F** are depth profiles of salinity (blue), fluorescence (green), and temperature (red) characteristic of each salinity category.

Hemiaulus hauckii without the endosymbiont, and *Pseudonitzchia* spp. were found in the region (A. Kalmbach and E. Carpenter pers. comm.). Other preliminary pigment results also support that this low-salinity plume region was dominated by coastal diatoms, although in lower abundance than during spring. In the plume station in the fall where microzooplankton and mesozooplankton grazing rates were both measured, the relative importance of mesozooplankton grazing was approximately four times higher than microzooplankton grazing (station 12 in Fig. 8).

From the patterns in grazing and phytoplankton assemblage, the inshore, coastal region of the plume can likely be characterized as a shorter, "export food web," with diatoms and mesozooplankton grazers prevalent (Michaels and Silver 1988; Legendre and Michaud 1998). Further support comes from previous reports of a similar pattern of phytoplankton distribution in the plume (Carpenter et al. 1999; Shipe et al. 2006; Subramaniam et al. 2008), as well as seasonal accumulation of calanoid copepods on the Amazon shelf corresponding to peak river discharge (Aller and Todorov 1997) which leads to a high biomass of coastal mesozooplankton grazers. The relatively lower importance of microzooplankton grazing rate compared with mesozooplankton in the inshore plume region (albeit measured from just one station) support this food web structure as well.

Mesohaline stations

During spring a large DDA bloom occurred between 9–14°N and 53–56°W throughout the mesohaline region. Goes et al. (2014) characterized the assemblage there as dominated by DDAs, but also with some dinoflagellates, cryptophytes, and *Trichodesmium*. However, mesozooplankton grazing rates in the same region were lower compared with the plume stations (Figs. 2A, 3B). In the fall the mesohaline stations were predominantly located in the outer arm of the plume during its seasonal retroflection (area of low salinity between 45 and 50°W in Fig. 3C) and characterized by diatoms, dinoflagellates, abundant *Synechococcus* spp., and very few DDAs. Given the largely different geographic regions of mesohaline stations, differences in grazing rates and phytoplankton assemblages may be unrelated or may be indicative of a seasonal succession (discussed below).

Comparison of the mesozooplankton and microzooplankton grazing impact in the mesohaline region suggests a

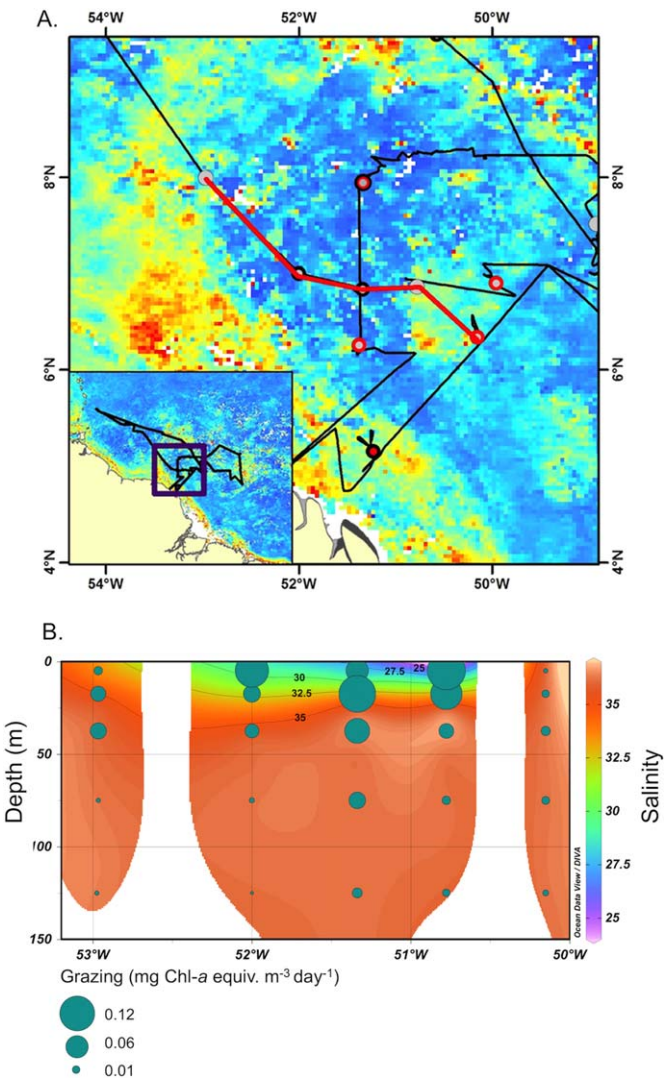

Fig. 5. Plume transect from the fall cruise (**A**; red line) and (**B**) depth profiles of salinity and mesozooplankton community grazing (green circles). Transect is overlaid on monthly averaged chromophoric dissolved organic matter (CDOM) concentration using Aqua-MODIS satellite data (oceancolor.gsfc.nasa.gov). The grazing depth profiles are plotted at the midpoint of the MOCNESS depth interval (i.e., 0–10 m is plotted at 5 m).

transition from an export food web to a retention food web (Fig. 8). Compared with lower salinities, between a SSS of 32–33 phytoplankton growth rates increase, as does the importance of microzooplankton grazing on the net change of phytoplankton biomass. At stations below 32 SSS, except for station 25, mesozooplankton grazing was higher than microzooplankton grazing (stations 12, 19, and 20), resulting in a negative net calculated change in phytoplankton (k'). At stations above 33 SSS, k' became positive and microzooplankton grazing impact dominated. Further sampling is required to determine if this transition consistently occurs over such a small salinity range.

In the mesohaline region in both seasons, mesozooplankton grazing rates in the furthest northwest station were elevated relative to adjacent mesohaline stations. In spring, the plume was distributed northwest toward the Caribbean, which may explain the observed elevated grazing there, but in fall the seasonal retroflection had occurred and adjacent stations were not Amazon plume-influenced. A potential explanation for enhanced grazing in this region during fall is influence from the Orinoco River plume, which has maximum discharge in August–November and flows north westward into the Caribbean and WTNA (Hellweger and Gordon 2002; Chérubin and Richardson 2007). Furthermore, a previous study in this region suggested a combination of the Amazon and Orinoco plumes supporting DDA blooms in this region (Carpenter et al. 1999).

Oceanic stations

On both cruises, mesozooplankton grazing rates were lowest in open ocean stations without plume influence. Higher mesozooplankton grazing impact on Chl *a* in the top 25 m at oceanic stations compared with lower salinity stations (Table 2) is best explained by low surface chlorophyll, rather than elevated grazing (Fig. 8C,F) at these stations. Higher rates of microzooplankton grazing compared with mesozooplankton occurred at oceanic stations with a phytoplankton assemblage comprised of *Trichodesmium, Synechococcus*, as well as some dinoflagellate species (Goes et al. unpubl.), supporting a "retention" food web. The average phytoplankton growth and microzooplankton grazing rates at oceanic stations ($\mu = 0.80$ d^{-1} and $m = 0.49$ d^{-1}, respectively, $n = 3$) as well as the higher salinity (SSS > 33) mesohaline stations ($\mu = 0.83$ d^{-1} and $m = 0.35$ d^{-1}, $n = 2$), compare well with the median value reported in the large meta-analysis of Schmoker et al. (2013) for the "Trades Atlantic" biogeographical subset ($\mu = 0.83$ d^{-1} and $m = 0.49$ d^{-1}; from Table 2 Schmoker et al. 2013), although the measurements for that region were restricted to the eastern Atlantic. Furthermore, ∂^{13}C data from the 2010 cruise showed an average 2.9‰ difference between particles and mesozooplankton at oceanic stations (Loicke-Wilde et al. in press), indicative of a complex microbial loop in the food web (Rau et al. 1990), but no significant difference at mesohaline or plume stations.

There was one exception in the spring where higher depth-integrated grazing occurred at an open ocean station compared with other oceanic stations and some mesohaline stations (Fig. 3B). Goes et al. (2014) characterized phytoplankton at that station as an oceanic assemblage comprised almost entirely of *Trichodesmium* and *Synechococcus* spp., although abundances of these cyanobacteria were not exceptionally high compared with other stations (see Fig. 6E,F from Goes et al. 2014). Based on this phytoplankton assemblage, elevated mesozooplankton grazing at this station is surprising as *Trichodesmium* is considered unpalatable to most mesozooplankton, with the exception of some

Table 2. Mesozooplankton grazing impact of all size fractions combined from 0–150 m and 0–25 m in spring (May–June) 2010 and fall (September–October) 2011. Values are average percentages ± 1 standard deviation for each year by station category and day or night tow. *Indicates a significant difference ($p < 0.05$) between years while † indicates a significant difference between station categories within given year.

		150 m Chl *a* impact		25 m Chl *a* impact	
Season	**Station category**	**Day**	**Night**	**Day**	**Night**
Spring	Low salinity plume	3.33 ± 5.47 ($n = 4$)	3.39 ($n = 1$)	2.08 ± 2.51 ($n = 4$)	7.18 ($n = 1$)
	Mesohaline plume	1.65 ± 1.89* ($n = 5$)	1.53 ± 0.92* ($n = 5$)	1.40 ± 1.76 ($n = 5$)	4.75 ± 2.61 ($n = 3$)
	Oceanic	1.94 ± 0.90 ($n = 4$)	2.08 ± 0.99 ($n = 3$)	4.28 ± 1.54 ($n = 4$)	4.94 ± 1.39 ($n = 3$)
	Total	2.26 ± 3.07 ($n = 13$)	1.92 ± 1.02 ($n = 9$)	2.49 ± 2.19 ($n = 13$)	5.18 ± 1.92 ($n = 7$)
Fall	Low salinity plume	11.70 ± 11.61 ($n = 4$)	9.37 ($n = 1$)	25.94 ± 25.50 ($n = 4$)	17.26 ($n = 1$)
	Mesohaline plume	6.44 ± 4.50* ($n = 13$)	7.19 ± 3.06*,† ($n = 7$)	21.69 ± 23.80 ($n = 13$)	17.01 ± 12.26 ($n = 7$)
	Oceanic	1.82 ($n = 2$)	2.16 ± 1.36† ($n = 3$)	4.16 ($n = 2$)	6.86 ± 3.76 ($n = 3$)
	Total	7.06 ± 6.65 ($n = 19$)	6.02 ± 3.54 ($n = 11$)	20.74 ± 22.88 ($n = 19$)	14.26 ± 10.75 ($n = 11$)

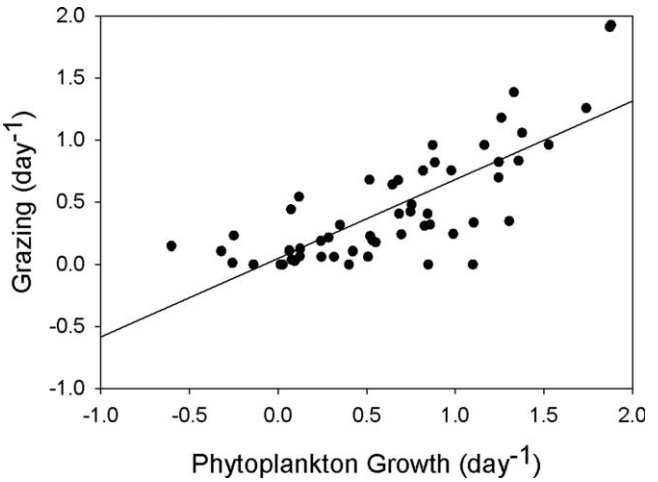

Fig. 6. Bulk phytoplankton growth vs. microzooplankton grazing rate across all salinity ranges. Microzooplankton grazing is significantly correlated with bulk phytoplankton growth rate ($R_2 = 0.602$, $p \leq 0.001$). Data are from two-point "mini" dilution experiments in fall.

harpactacoid copepods (Hawser et al. 1992; O'Neil and Roman 1994; O'Neil 1998). Mesozooplankton grazing on *Synechococcus* individuals has been documented (Gorsky et al. 1999; Stukel et al. 2013a), or mesozooplankton may consume *Synechococcus* via feeding on aggregates (Wilson and Steinberg 2010). Analysis of zooplankton gut contents for phycoerythrin, a diagnostic pigment for *Synechococcus*, and cyanobacteria molecular markers will help determine direct consumption by zooplankton (Conroy et al. unpubl.). Aside from this exception in 2010, the grazing patterns of meso- and microzooplankton at oceanic stations support a "retention" style food web dominated by microzooplankton rather than mesozooplankton.

Vertical patterns

To our knowledge this is the first grazing study to utilize a depth-stratified sampling design using the MOCNESS, which enabled us to investigate how the strong salinity gradient in the upper water column created by the plume influenced grazing with depth. Depth profiles of grazing at plume and mesohaline stations indicated highest grazing in the surface 25 m in plume-influenced waters, while at oceanic stations grazing was higher at depth. This pattern largely followed Chl *a* profiles, with deeper grazing in oceanic stations in particular reflecting the deep Chl *a* maximum. Slightly reduced grazing rates for some size fractions in the surface 10 m (compared with 10–25 m) at all stations may reflect feeding avoidance in surface waters with more intense solar radiation (Alonso et al. 2004). Finally, depth-stratified sampling is a useful approach for grazing studies in a region with pronounced vertical physical structure, and our integrated grazing rates fall within the range of similar grazing studies using non-stratified sampling (e.g., Huskin et al. 2001; Isla et al. 2004; Décima et al. 2011).

Diel patterns

We expected higher nighttime grazing impact due to additional feeding in surface waters by diel vertical migrators at night, but interestingly, nighttime grazing impact across all salinities was similar to daytime. Vertical migrators thus may have been preying on small invertebrates rather than primary producers, a pattern observed in the Sargasso Sea (Schnetzer and Steinberg 2002). Alternatively, at least in the plume, PAR profiles indicated that incident light was rapidly attenuated to 15% of surface irradiance within the top 2–8 m, rendering day light conditions more similar to night in plume waters, resulting in a lack of a diel pattern in grazing impact.

Seasonal comparison

ANACONDAS was designed to provide seasonal snapshots of the Amazon Plume region with a focus on the fate of DDAs. While the seasons were sampled in two different

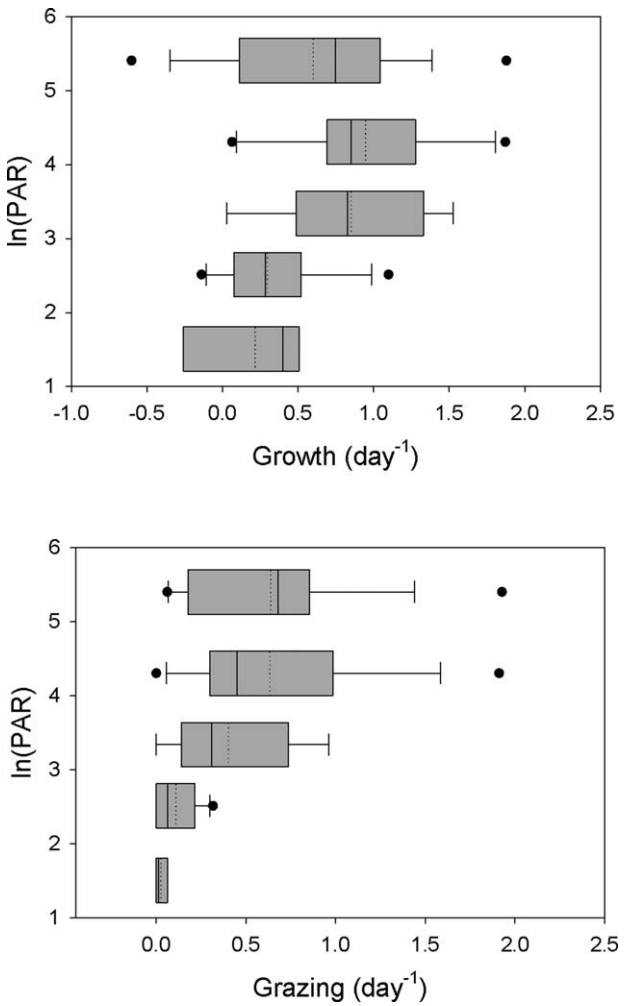

Fig. 7. Natural logarithm of photosynthetically active radiation (PAR) vs. bulk phytoplankton growth (**A**) and microzooplankton grazing (**B**) in fall. Box boundaries represent the 25th and 75th percentiles. The solid line is the median while the dashed is the mean. Whiskers represent the 10th and 90th percentiles. Maximum phytoplankton growth rates occur at intermediate PAR levels corresponding to irradiances of roughly 10% surface irradiance.

years, the overall patterns provide some insight into planktonic succession and functioning of the food web in the region. In the lowest salinity plume stations in both spring and fall, phytoplankton assemblages are consistent with previous reports in low salinity, inshore regions of the plume. After initial low biomass at the mouth of the Amazon River due to light limitation (Smith and Demaster 1996), biomass increases further offshore and comprises mostly coastal diatoms (Smith and Demaster 1996; Subramaniam et al. 2008; Goes et al. 2014). Despite similar coastal phytoplankton assemblages at plume stations in both years, mesozooplankton grazing rates and impact on Chl *a* were higher in the fall than spring. We view this as a seasonal rather than an interannual signal, and a reflection of a lag in the increase in mesozooplankton grazing and biomass following peak discharge. A similar explanation was used to describe the initial lag in copepod grazing on the phytoplankton bloom associated with the Mississippi River plume entering the Gulf of Mexico (Dagg 1995). They reported copepod grazing of 4–5% of daily production in the late spring during the onset of the phytoplankton bloom compared with 14–62% when the Mississippi plume was sampled in the late summer. This pattern is similar in our study (See Table 2). This is also supported by overall higher plume mesozooplankton biomass observed in fall compared with spring (Steinberg et al. unpubl.). While a seasonal bloom is counter to the steady year-round productivity in the plume seen by Demaster and Pope (1996) discussed above, it is important to note the differences in distance from the mouth of the Amazon. Almost all of their stations were in shallow water (majority were < 100 m with max ~ 200 m bottom depth) while ANACONDAS was further north of the mouth and focused on the slope and offshore regions of the plume-influenced WTNA. Therefore, a seasonal bloom progression may be important in the offshore plume waters as the Amazon progresses through peak discharge in the late spring, while inshore and closer to the mouth primary productivity is steady year round as observed by Demaster and Pope (1996). Loick-Wilde et al. (in press) suggest that the inshore phytoplankton assemblage acts as a seed population for blooms in the outer plume, especially of DDAs in the mesohaline region, which would support a seasonal progression of increasing phytoplankton biomass followed by zooplankton in the outer plume.

Furthermore, higher grazing rates and grazing impact occurred later in the season (higher in fall than spring) at plume and mesohaline stations (see Tables 1, 2), supporting an initial lag in mesozooplankton growth and grazing before they are able to catch up to the pulse of primary production. However, in contrast to the plume region where phytoplankton assemblages were similar between seasons, in spring a DDA bloom appeared to have just initiated, based on cell condition (E. Carpenter and R. Foster pers. comm.), and DDAs were prevalent throughout the mesohaline, while in the fall DDAs were scarce. Lower grazing in the spring may thus alternatively be due to intense grazing by zooplankton on DDAs later in the fall; stable isotope analysis indicated diazotrophic nitrogen was incorporated into mesozooplankton during our and a previous study in the region (Montoya et al. 2002) as well as in the subtropical Atlantic (Landrum et al. 2011), although direct grazing on DDAs is not distinguishable using this method.

An alternative explanation for lower grazing in spring is that mesozooplankton avoid grazing on DDAs, and the high abundances of DDAs suppressed grazing. The DDA bloom observed in spring was dominated by the diatom *Hemiaulus hauckii* with the endosymbiont *Richelia intracellularis*,

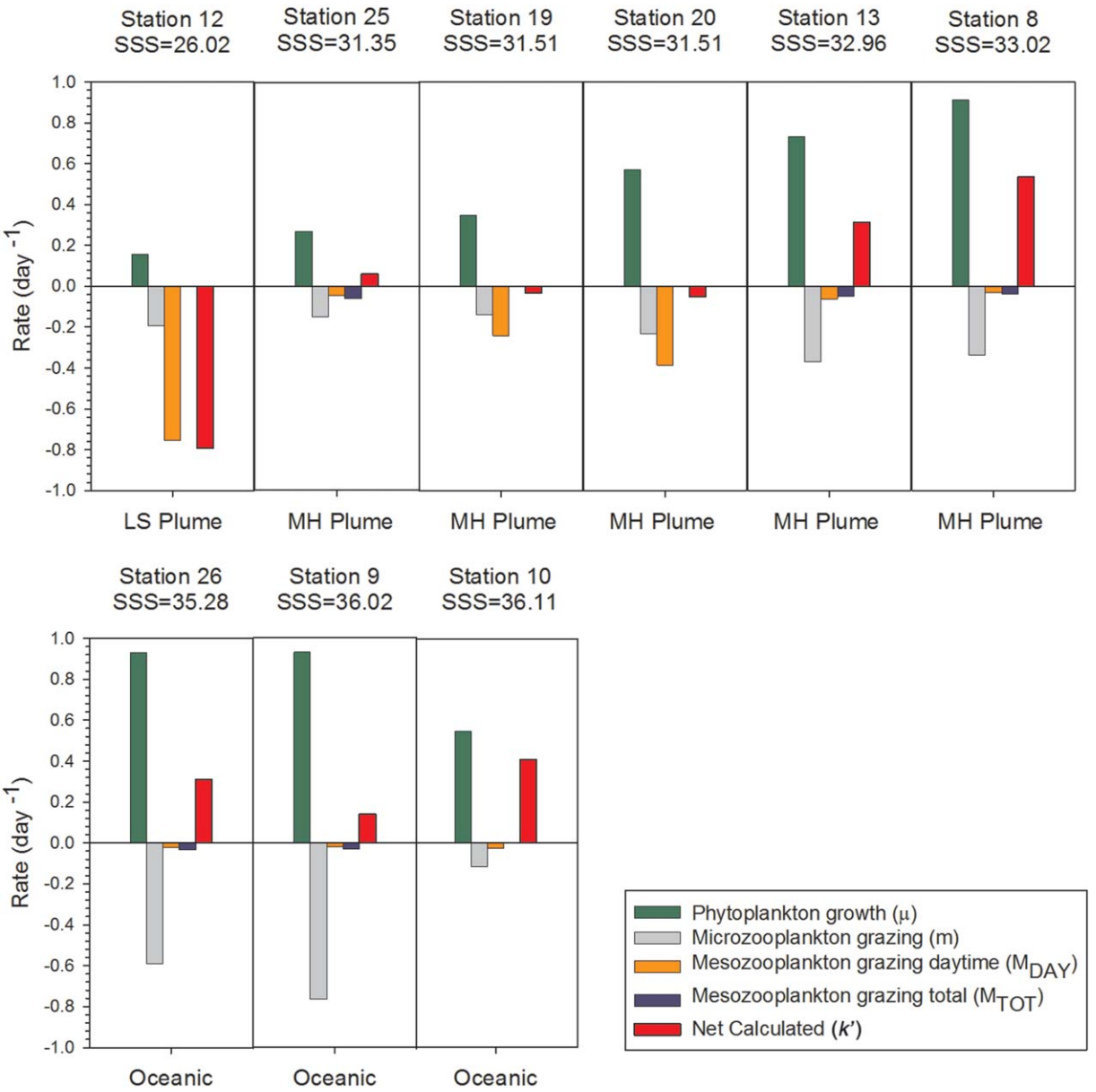

Fig. 8. Instantaneous rates of change for phytoplankton growth (μ), microzooplankton grazing (m), and mesozooplankton total grazing (M_{TOT}) or daytime mesozooplankton (M_{DAY}) in fall. The net calculated change k' is equal to μ-m-M_{TOT} (or M_{DAY} for Sts. 10, 12, 19, and 20 where no night tow was performed).

although *Rhizosolenia clevei* with *R. intracellularis* was present as well (Goes et al. 2014). Chain-formation in diatoms such as *Hemiaulus* and *Rhizosolenia* may decrease the risk of being grazed (Bergkvist et al. 2012), however, similar sized chain-forming diatoms are actively grazed by copepods (Bochdansky and Bollens 2004) and stable isotope analysis of mesozooplankton sampled in spring and fall indicates diazotrophic nitrogen in both seasons (Loicke-Wilde et al. in press). These observations suggest mesozooplankton do not avoid DDAs, but instead relate to a pattern of seasonal planktonic progression in the plume, especially in the mesohaline region where DDA blooms are more prevalent (Subramaniam et al. 2008; Goes et al. 2014).

Summary and conclusions

We present the first analysis of zooplankton grazing in the Amazon Plume-influenced WTNA. Results from both years indicate that the Amazon Plume enhances grazing in the WTNA compared to areas with no plume influence. A shift in food web structure occurs along the plume salinity gradient, with mesozooplankton dominating grazing in plume and low

salinity mesohaline stations, suggestive of an export food web, transitioning to microzooplankton dominating grazing at higher salinity mesohaline (> 33 SSS) and oceanic stations, and a retention food web. Comparison between the two seasons/years indicated lower mesozooplankton grazing during peak spring discharge compared with the fall retroflection phase of the plume. This pattern represents a seasonal phytoplankton-zooplankton progression in the outer plume through peak discharge into the retroflection period. During the onset of a bloom in mesohaline waters, mesozooplankton grazing appears to lag phytoplankton growth, before catching up and grazing down the bloom, by the fall retroflection phase.

This study also provides an important baseline of zooplankton grazing impact in the WTNA with regards to a changing climate. Elevated precipitation and evaporation rates, driven by warming atmospheric and ocean temperatures, (Doney et al. 2012) would directly affect the expanse of the plume into the WTNA, potentially altering the food web dynamics highlighted in this study. Some changes have already been observed in the hydrological cycle of the Amazon basin over the last two decades, with an increased wetting trend driving an increase in annual river discharge (Gloor et al. 2013). A warming ocean will increase stratification, decreasing nutrient flux from depth (Doney et al. 2012); under these conditions N_2-fixation may increase in importance, making diazotrophy important in fueling secondary production. Furthermore, our estimates of grazing can be incorporated into existing biogeochemical models for this region (Cooley et al. 2007; Stukel et al. 2014) to understand how changes in precipitation, temperature, or other factors may impact biogeochemical cycling, and to predict energy transfer in future ocean food webs.

References

Aller, J. Y., and J. R. Todorov. 1997. Seasonal and spatial patterns of deeply buried calanoid copepods on the Amazon Shelf: Evidence for periodic erosional/depositional cycles. Estuar. Coast. Shelf Sci. **44**: 57–66. doi:10.1006/ecss.1996.0111

Alonso, C., V. Rocco, J. P. Barriga, M. A. Battini, and H. Zagarese. 2004. Surface avoidance by freshwater zooplankton: Field evidence on the role of ultraviolet radiation. Limnol. Oceanogr. **49**: 225–232. doi:10.4319/lo.2004.49.1.0225

Båmstedt, U., D. J. Gifford, X. Irigoien, A. Atkinson, and M. Roman. 2000. Feeding, p. 297–399. *In* R. P. Harris, P. H. Wiebe, J. Lenz, H. R. Skjodal and M. Huntley [eds.], ICES zooplankton methodology manual. Elsevier Academic Press.

Bergkvist, J., P. Thor, H. Henrik Jakobsen, S.-Å. Wängberg, and E. Selander. 2012. Grazer-induced chain length plasticity reduces grazing risk in a marine diatom. Limnol. Oceanogr. **57**: 318. doi:10.4319/lo.2012.57.1.0318

Bernard, K. S., D. K. Steinberg, and O. M. E. Schofield. 2012. Summertime grazing impact of the dominant macrozooplankton off the Western Antarctic Peninsula. Deep-Sea Res. Part Oceanogr. Res. Pap. **62**: 111–122. doi:10.1016/j.dsr.2011.12.015

Bochdansky, A. B., and S. M. Bollens. 2004. Relevant scales in zooplankton ecology: Distribution, feeding, and reproduction of the copepod *Acartia hudsonica* in response to thin layers of the diatom *Skeletonema costatum*. Limnol. Oceanogr. **49**: 625–636. doi:10.4319/lo.2004.49.3.0625

Calbet, A., and M. R. Landry. 2004. Phytoplankton growth, microzooplankton grazing, and carbon cycling in marine systems. Limnol. Oceanogr. **49**: 51–57. doi:10.4319/lo.2004.49.1.0051

Calef, G. F., and G. D. Grice. 1967. Influence of the Amazon River outflow on the ecology of the Western Tropical Atlantic II. Zooplankton abundance, copepod distribution, with remarks on the fauna of low-salinity areas. J. Mar. Res. **25**: 84–92.

Carpenter, E. J., J. P. Montoya, J. Burns, M. R. Mulholland, A. Subramaniam, and D. G. Capone. 1999. Extensive bloom of a N_2-fixing diatom/cyanobacterial association in the tropical Atlantic Ocean. Marine Ecology Progress Series. **185**: 273–283

Chérubin, L. M., and P. L. Richardson. 2007. Caribbean current variability and the influence of the Amazon and Orinoco freshwater plumes. Deep-Sea Res. Part Oceanogr. Res. Pap. **54**: 1451–1473. doi:10.1016/j.dsr.2007.04.021

Coles, V. J., M. T. Brooks, J. Hopkins, M. R. Stukel, P. L. Yager, and R. R. Hood. 2013. The pathways and properties of the Amazon River Plume in the tropical North Atlantic Ocean: Amazon River plume. J. Geophys. Res. Oceans **118**: 6894–6913. doi:10.1002/2013JC008981

Conover, R. J., R. Durvasula, S. Roy, and R. Wang. 1986. Probable loss of chlorophyll-derived pigments during passage through the gut of zooplankton, and some of the consequences. Limnol. Oceanogr. **31**: 878–887. doi:10.4319/lo.1986.31.4.0878

Cooley, S. R., and P. L. Yager. 2006. Physical and biological contributions to the western tropical North Atlantic Ocean carbon sink formed by the Amazon River plume. J. Geophys. Res. **111**. doi:10.1029/2005JC002954

Cooley, S. R., V. J. Coles, A. Subramaniam, and P. L. Yager. 2007. Seasonal variations in the Amazon plume-related atmospheric carbon sink: Seasonality of CO_2 in Amazon plume. Glob. Biogeochem. Cycles **21**: GB3014. doi:10.1029/2006GB002831

Costa, R. M., N. R. Leite, and L. C. C. Pereira. 2009. Mesozooplankton of the Curuçá Estuary (Amazon Coast, Brazil). J. Coast. Res. **56**: 400–404.

Dagg, M. J. 1995. Copepod grazing and the fate of phytoplankton in the northern Gulf of Mexico. Cont. Shelf Res. **15**: 1303–1317. doi:10.1016/0278-4343(94)00086-3

Dam, H. G., and W. T. Peterson. 1988. The effect of temperature on the gut clearance rate constant of planktonic

copepods. J. Exp. Mar. Biol. Ecol. **123**: 1–14. doi:10.1016/0022-0981(88)90105-0

Dam, H. G., X. Zhang, M. Butler, and M. R. Roman. 1995. Mesozooplankton grazing and metabolism at the equator in the central Pacific: Implications for carbon and nitrogen fluxes. Deep-Sea Res. Part II Top. Stud. Oceanogr. **42**: 735–756. doi:10.1016/0967-0645(95)00036-P

Décima, M., M. R. Landry, and R. R. Rykaczewski. 2011. Broad scale patterns in mesozooplankton biomass and grazing in the eastern equatorial Pacific. Deep-Sea Res. Part II Top. Stud. Oceanogr. **58**: 387–399. doi:10.1016/j.dsr2.2010.08.006

Demaster, D. J., and R. H. Pope. 1996. Nutrient dynamics in Amazon shelf waters: Results from AMASSEDS. Cont. Shelf Res. **16**: 263–289. doi:10.1016/0278-4343(95)00008-O

Doney, S. C., and others. 2012. Climate change impacts on marine ecosystems. Annu. Rev. Mar. Sci. **4**: 11–37. doi:10.1146/annurev-marine-041911-111611

Durbin, E. G., and R. G. Campbell. 2007. Reassessment of the gut pigment method for estimating in situ zooplankton ingestion. Mar. Ecol. Prog. Ser. **331**: 305–307. doi:10.3354/meps331305

Espinoza, J. C., and others. 2011. Climate variability and extreme drought in the upper Solimões River (western Amazon Basin): Understanding the exceptional 2010 drought. Geophys. Res. Lett. **38**: L13406. doi:10.1029/2011GL047862

Gannon, J. E., and S. A. Gannon. 1975. Observations on the narcotization of crustacean zooplankton. Crustaceana **28**: 220–224. doi:10.1163/156854075X00775

Gleiber, M. R., D. K. Steinberg, and O. M. E. Schofield. 2015. Copepod summer grazing and fecal pellet production along the Western Antarctic Peninsula. J. Plankton Res. doi:10.1093/plankt/fbv070

Gloor, M., and others. 2013. Intensification of the Amazon hydrological cycle over the last two decades: Amazon hydrologic cycle intensification. Geophys. Res. Lett. **40**: 1729–1733. doi:10.1002/grl.50377

Goes, J. I., and others. 2014. Influence of the Amazon River discharge on the biogeography of phytoplankton communities in the western tropical north Atlantic. Prog. Oceanogr. **120**: 29–40. doi:10.1016/j.pocean.2013.07.010

Gorsky, G., M. J. Chrétiennot-Dinet, J. Blanchot, and I. Palazzoli. 1999. Picoplankton and nanoplankton aggregation by appendicularians: Fecal pellet contents of *Megalocercus huxleyi* in the equatorial Pacific. J. Geophys. Res. Oceans **104**: 3381–3390. doi:10.1029/98JC01850

Hawser, S. P., J. M. O'neil, M. R. Roman, and G. A. Codd. 1992. Toxicity of blooms of the cyanobacterium *Trichodesmium* to zooplankton. J. Appl. Phycol. **4**: 79–86. doi:10.1007/BF00003963

Hellweger, F. L., and A. L. Gordon. 2002. Tracing Amazon River water into the Caribbean Sea. J. Mar. Res. **60**: 537–549. doi:10.1357/002224002762324202

Hopcroft, R. R., J. C. Roff, and F. P. Chavez. 2001. Size paradigms in copepod communities: A re-examination. Hydrobiologia **453**: 133–141. doi:10.1007/0-306-47537-5_11

Huskin, I., R. Anadón, G. Medina, R. N. Head, and R. P. Harris. 2001. Mesozooplankton distribution and copepod grazing in the subtropical Atlantic near the Azores: Influence of mesoscale structures. J. Plankton Res. **23**: 671–691. doi:10.1093/plankt/23.7.671

Isla, J. A., M. Llope, and R. Anadón. 2004. Size-fractionated mesozooplankton biomass, metabolism and grazing along a 50°N–30°S transect of the Atlantic Ocean. J. Plankton Res. **26**: 1301–1313. doi:10.1093/plankt/fbh121

Karaköylü, E. M., and P. J. S. Franks. 2012. Reassessment of copepod grazing impact based on continuous time series of in vivo gut fluorescence from individual copepods. J. Plankton Res. **34**: 55–71. doi:10.1093/plankt/fbr086

Knap, A. H., A. Michaels, A. R. Close, H. Ducklow, and A. G. Dickson. 1996. Protocols for the joint global ocean flux study (JGOFS) core measurements. JGOFS Repr. IOC Man. Guid. No 29 UNESCO 1994 19.

Landrum, J. P., M. A. Altabet, and J. P. Montoya. 2011. Basin-scale distributions of stable nitrogen isotopes in the subtropical North Atlantic Ocean: Contribution of diazotroph nitrogen to particulate organic matter and mesozooplankton. Deep-Sea Res. Part Oceanogr. Res. Pap. **58**: 615–625. doi:10.1016/j.dsr.2011.01.012

Landry, M. R., and R. P. Hassett. 1982. Estimating the grazing impact of marine micro-zooplankton. Mar. Biol. **67**: 283–288. doi:10.1007/BF00397668

Landry, M., L. Haas, and V. Fagerness. 1984. Dynamics of microbial plankton communities. Mar. Ecol. Prog. Ser. **16**: 127–133. doi:10.3354/meps016127

Landry, M. R., S. L. Brown, Y. M. Rii, K. E. Selph, R. R. Bidigare, E. J. Yang, and M. P. Simmons. 2008. Depth-stratified phytoplankton dynamics in Cyclone Opal, a subtropical mesoscale eddy. Deep-Sea Res. Part II Top. Stud. Oceanogr. **55**: 1348–1359. doi:10.1016/j.dsr2.2008.02.001

Landry, M. R., M. D. Ohman, R. Goericke, M. R. Stukel, and K. Tsyrklevich. 2009. Lagrangian studies of phytoplankton growth and grazing relationships in a coastal upwelling ecosystem off Southern California. Prog. Oceanogr. **83**: 208–216. doi:10.1016/j.pocean.2009.07.026

Landry, M. R., K. E. Selph, A. G. Taylor, M. Décima, W. M. Balch, and R. R. Bidigare. 2011. Phytoplankton growth, grazing and production balances in the HNLC equatorial Pacific. Deep-Sea Res. Part II Top. Stud. Oceanogr. **58**: 524–535. doi:10.1016/j.dsr2.2010.08.011

Legendre, L., and J. Michaud. 1998. Flux of biogenic carbon in oceans: Size-dependent regulation by pelagic food webs. Mar. Ecol. Prog. Ser. **164**: 1–11. doi:10.3354/meps164001

Loick-Wilde, N., and others. In press. Nitrogen sources and net growth efficiency of zooplankton in three Amazon

River plume food webs. Limnol. Oceanogr. doi:10.1002/lno.10227V

Magalhães, A., N. da R. Leite, J. G. Silva, L. C. Pereira, and R. M. da Costa. 2009. Seasonal variation in the copepod community structure from a tropical Amazon estuary, Northern Brazil. An. Acad. Bras. Ciênc. **81**: 187–197. doi:10.1590/S0001-37652009000200005

Michaels, A. F., and M. W. Silver. 1988. Primary production, sinking fluxes and the microbial food web. Deep-Sea Res. Part Oceanogr. Res. Pap. **35**: 473–490. doi:10.1016/0198-0149(88)90126-4

Mikaloff Fletcher, S. E., and others. 2007. Inverse estimates of the oceanic sources and sinks of natural CO_2 and the implied oceanic carbon transport: Natural air-sea fluxes of CO_2. Glob. Biogeochem. Cycles **21**: GB1010. doi:10.1029/2006GB002751

Molleri, G. S. F., E. M. L. d. M. Novo, and M. Kampel. 2010. Space-time variability of the Amazon River plume based on satellite ocean color. Cont. Shelf Res. **30**: 342–352. doi:10.1016/j.csr.2009.11.015

Montoya, J. P., E. J. Carpenter, and D. G. Capone. 2002. Nitrogen fixation and nitrogen isotope abundances in zooplankton of the oligotrophic North Atlantic. Limnol. Oceanogr. **47**: 1617–1628. doi:10.4319/lo.2002.47.6.1617

O'Neil, J. M. 1998. The colonial cyanobacterium *Trichodesmium* as a physical and nutritional substrate for the harpacticoid copepod *Macrosetella gracilis*. J. Plankton Res. **20**: 43–59. doi:10.1093/plankt/20.1.43

O'Neil, J. M., and M. R. Roman. 1994. Ingestion of the cyanobacterium *Trichodesmium* spp. by pelagic harpacticoid copepods Macrosetella, Miracia and Oculosetella. Hydrobiologia **292**: 235–240. doi:10.1007/BF00229946

Parsons, T. R., Y. Maita, and C. M. Lalli. 1984. A manual of chemical and biological methods for seawater analysis. Pergamon Press.

Rau, G. H., J.-L. Teyssie, F. Rassoulzadegan, and S. W. Fowler. 1990. 13C/12C and 15N/14N variations among size-fractionated marine particles: Implications for their origin and trophic relationships. Mar. Ecol. Prog. Ser. **59**: 33–38. doi:10.3354/meps059033

Richey, J. E., C. Nobre, and C. Deser. 1989. Amazon River discharge and climate variability. Science **246**: 101–103. doi:10.1126/science.246.4926.101

Roman, M. R., and A. L. Gauzens. 1997. Copepod grazing in the equatorial Pacific. Limnol. Oceanogr. **42**: 623–634. doi:10.4319/lo.1997.42.4.0623

Roman, M. R., H. G. Dam, R. Le Borgne, and X. Zhang. 2002. Latitudinal comparisons of equatorial Pacific zooplankton. Deep-Sea Res. Part II Top. Stud. Oceanogr. **49**: 2695–2711. doi:10.1016/S0967-0645(02)00054-1

Schmoker, C., S. Hernández-León, and A. Calbet. 2013. Microzooplankton grazing in the oceans: Impacts, data variability, knowledge gaps and future directions. J. Plankton Res. **35**: 691–706. doi:10.1093/plankt/fbt023

Schnetzer, A., and D. Steinberg. 2002. Natural diets of vertically migrating zooplankton in the Sargasso Sea. Mar. Biol. **141**: 89–99. doi:10.3354/meps234071

Sherr, E. B., and B. F. Sherr. 2002. Significance of predation by protists in aquatic microbial food webs. Antonie Van Leeuwenhoek **81**: 293–308. doi:10.1023/A:1020591307260

Shipe, R. F., J. Curtaz, A. Subramaniam, E. J. Carpenter, and D. G. Capone. 2006. Diatom biomass and productivity in oceanic and plume-influenced waters of the western tropical Atlantic ocean. Deep-Sea Res. Part Oceanogr. Res. Pap. **53**: 1320–1334. doi:10.1016/j.dsr.2006.05.013

Smith, W. O., Jr., and D. J. Demaster. 1996. Phytoplankton biomass and productivity in the Amazon River plume: Correlation with seasonal river discharge. Cont. Shelf Res. **16**: 291–319. doi:10.1016/0278-4343(95)00007-N

Stukel, M. R., M. Décima, K. E. Selph, D. A. A. Taniguchi, and M. R. Landry. 2013a. The role of *Synechococcus* in vertical flux in the Costa Rica upwelling dome. Prog. Oceanogr. **112–113**: 49–59. doi:10.1016/j.pocean.2013.04.003

Stukel, M. R., M. D. Ohman, C. R. BenitezNelson, and M. R. Landry. 2013b. Contributions of mesozooplankton to vertical carbon export in a coastal upwelling system. Mar. Ecol. Prog. Ser. **491**: 47–65. doi:10.3354/meps10453

Stukel, M. R., V. J. Coles, M. T. Brooks, and R. R. Hood. 2014. Top-down, bottom-up and physical controls on diatom-diazotroph assemblage growth in the Amazon River plume. Biogeosciences **11**: 3259–3278. doi:10.5194/bg-11-3259-2014

Subramaniam, A., and others. 2008. Amazon River enhances diazotrophy and carbon sequestration in the tropical North Atlantic Ocean. Proc. Natl. Acad. Sci. USA **105**: 10460–10465. doi:10.1073/pnas.0710279105

Takahashi, T., and others. 2002. Global sea–air CO_2 flux based on climatological surface ocean pCO_2, and seasonal biological and temperature effects. Deep-Sea Res. Part II Top. Stud. Oceanogr. **49**: 1601–1622. doi:10.1016/S0967-0645(02)00003-6

Wassmann, P. 1997. Retention versus export food chains: Processes controlling sinking loss from marine pelagic systems. Hydrobiologia **363**: 29–57. doi:10.1023/A:1003113403096

Wiebe, P. H., K. H. Burt, S. H. Boyd, and A. W. Morton. 1976. A multiple opening/closing net and environmental sensing system for sampling zooplankton. J. Mar. Res. **34b**: 313–326.

Wilson, S., and D. Steinberg. 2010. Autotrophic picoplankton in mesozooplankton guts: Evidence of aggregate feeding in the mesopelagic zone and export of small phytoplankton. Mar. Ecol. Prog. Ser. **412**: 11–27. doi:10.3354/meps08648

Zhang, X., H. G. Dam, J. R. White, and M. R. Roman. 1995. Latitudinal variations in mesozooplankton grazing and metabolism in the central tropical Pacific during the U.S. JGOFS EqPac study. Deep-Sea Res. Part II Top. Stud. Oceanogr. **42**: 695–714. doi:10.1016/0967-0645(95)00032-L

Acknowledgment

We would like to thank the captain, officers, and crew of both the R/V *Knorr* and R/V *Melville* for their support and hard work during both cruises. We are grateful to Joe Cope, Miram Gleiber, Joshua Stone, and Jason Landrum for their help in sample collection and processing at sea, and to Jenna Luek and Anya Voloshin for their assistance with chlorophyll analysis at our home institution. Special thanks to Chief Scientist and Lead PI Patricia Yager for her leadership of the ANACONDAS project, and to all of our other ANACONDAS collaborators. This research was funded by National Science Foundation grants OCE-0934036 to D. Steinberg, NSF-OCE-1133277 to J. Goes, and NSF-OCE-0933975 to V. Coles. This is contribution number 3521 from the Virginia Institute of Marine Science.

Submitted 26 May 2015
Revised 22 October 2015
Accepted 30 November 2015

Associate editor: Thomas Kiørboe